IIETA International Information and Engineering Technology Association
Advancing the World of Information and Engineering

Mathematical Modelling of Engineering Problems
Vol. 12, No. 8, August, 2025, pp. 2899-2907
Journal homepage: http://iieta.org/journals/mmep

Finite Element Simulation of Fatigue Performance and Microhardness in Friction Stir Welded AA2024 with Y_2O_3 Nanoparticles

Abbas Nasser Hasein*, Duaa Abbas Falih, Mortadha Kareem A. Razzaq

Kut Technical Institution, Middle Technical University, Baghdad 10074, Iraq

Corresponding Author Email: Abbasn.hasein@mtu.edu.iq

https://doi.org/10.18280/mmep.120831

Received: 15 March 2025
Revised: 25 June 2025
Accepted: 4 July 2025
Available online: 31 August 2025

Keywords:
fatigue, microhardness, nano-Y_2O_3, aluminum alloy 2024, finite element analysis (FEA), friction stir welding (FSW), ANSYS Workbench

ABSTRACT

This work investigates the fatigue performance and microhardness distribution of friction stir welded aluminum alloy 2024 reinforced by nano-Y_2O_3. Finite element analysis (FEA) via ANSYS Workbench was used to evaluate the equivalent stress, fatigue life prediction, and microhardness differences throughout the base metal (BM), heat-affected zone (HAZ), and weld zone. While fatigue life was assessed through simulation, experimental validation was conducted using microhardness data for both Nano-reinforced and non-reinforced joints at a speed of welding of 24 mm/min and a speed of rotation 1525 rpm. Additionally, optical microscopy was employed for microstructural investigation to examine phase distribution and grain refinement in different weld regions. The results show that by lowering stress concentrations and enhancing microhardness, nano-Y_2O_3 reinforcement improves the weldment's predicted fatigue performance and mechanical stability. Given the enhanced performance, nano-Y_2O_3 appears to be a promising reinforcement material for high-performance structural and aeronautical applications.

1. INTRODUCTION

Due to its good mechanical properties, resistance of corrosion, electrical and thermal conductivity, and perfect technological properties, alloys of aluminum are mostly used in various fields such as automobile, aerospace, military, and structural [1-4]. Aerospace industry often uses AA2024 in stringers and fuselage in the aircraft wings to produce light-weight frame. Conventional joining processes like welding, riveting, and bolting are unavoidable to product large structures. However, use of bolts and rivets for construct large structures deteriorates the structural integrity and adds to the total weight. These disadvantages can be defeat by using conventional welding processes. Though, the weldability of these high strength aluminum alloys using conventional welding processes is extremely poor with depleted fatigue life and low efficiency [5-10]. Friction stir welding (FSW), is a solid-state method has been developed for these alloys [11]. FSW is a well-known method of combining aluminum alloys because it produces welds that are high quality and have few flaws. Nonetheless, a major area of concern continues to be the fatigue performance of FSW joints, particularly when considering the cyclic loading conditions commonly found in aerospace applications [12, 13]. A lot of research has been done in the last few years, on the behavior of fatigue joints of FSW [14-19]. There is agreement that fatigue behavior of welded joints is lesser than that base material (BM) [20, 21].

To develop the mechanical properties of FSW joints, use of nanoscale reinforcements has gained increased attention recently, because of its capacity to enhance the thermal stability of welded joints and refine grain architectures [22-25]. Many researchers have studied the influences of nanoparticles addition on welded joints mechanical properties [26-30]. The investigation by Asl et al. [26] investigates the different joining of alloy sheets of magnesium and aluminum using FSW with TiO_2 nanoparticles. The weld joints were designed with a groove to prevent nanoparticle dissipation. Results showed that nanoparticles significantly increased tensile strength and microhardness of welded joints. Shehabeldeen et al. [27] studied how nano γ-Al_2O_3 nano powder affected the mechanical characteristics, weldability and microstructure of FSW lap joint of AA6061-T6 and Ti6Al4V. They found that there were notable improvements in FSW properties of Al/Ti joints. Kamaleshwar et al. [28] in their study, the composite of AA3003 surface is synthesized by reinforcement nano-Y_2O_3 particles into the matrix composed with friction stir processing (FSP). Optimal FSP parameters for welding of AA3003-Y_2O_3 surface composite are found. The particles of nano-Y_2O_3 influence on mechanical characteristic and microstructure is comprehensively analyzed. From the results, after FSP the strength and hardness of surface composite sample were improved, due to the regularly distribution of reinforcement Y_2O_3 in AA3003 matrix. Zhu et al. [29] studied how Al3 (Sc1−xZrx) nanoparticles influence the microstructure and mechanical properties of FSW Al−Mg−Mn alloys. Theoretical analysis suggests that these nanoparticles contribute to grain boundary reinforcement in weld zone, enhancing the strength of yield for the Al−Mg−Mn joint by 97 MPa. Yaghoubi et al. [30] investigated the effects of FSP on severely deformed pure Cu

sheets, with and without yttria nanoparticles. Yttria addition prevented rapid grain growth, leading to finer grains, higher hardness, and improved strength and wear resistance.

All of these investigations and others point to the potential of significantly improving the behavior of fatigue for FSW joints through the use of nano-reinforcement. While several studies have explored various alloys and nanoparticle additions such as Al_2O_3 in AA6061 [27] and Y_2O_3 in AA3003 [28] the direct impact of Y_2O_3 nanoparticles on the performance of fatigue for friction stir welded AA2024 under cyclic and aerospace-relevant loading conditions remains underexplored. This work therefore aims to address that specific knowledge gap by evaluating how Y_2O_3 reinforcement influences both fatigue behavior and microhardness in AA2024 FSW joints. By conducting a comprehensive finite element fatigue analysis alongside experimental validation of microstructure and hardness, this study offers a focused contribution on a material widely used in aircraft structures, where long-term cyclic performance is critical. Thus, it advances the current literature by specifically targeting AA2024 with Y_2O_3 under loading conditions pertinent to real-world aerospace environments.

2. METHODOLOGY

2.1 Material and welding process

In the applications of aerospace Aluminum alloy 2024 is usually used because it has 73 GPa (10.6 Msi) Young's Modulus, 30% electrical conductivity IACS, 2.78 g/cm^3 (0.1 lb/in3) density, and has chemical composition as in Table 1. Two sets of aluminum plates were subjected to FSW technique. First set was welded without using of nanoparticles, while the other set was welded using nano-Y_2O_3 particles added to weld zone.

Table 1. Typical chemical composition of aluminum 2024 (in % by weight)

Element	Minimum (%)	Maximum (%)
Aluminum (Al)	Balance	Balance
Copper (Cu)	3.8	4.9
Magnesium (Mg)	1.2	1.8
Manganese (Mn)	0.3	0.9
Iron (Fe)	—	0.50
Silicon (Si)	—	0.50
Zinc (Zn)	—	0.25
Titanium (Ti)	—	0.15
Chromium (Cr)	—	0.10
Other elements (each)	—	0.05
Other elements (total)	—	0.15

2.2 FSW process

FSW was used to join two sets of 2024 aluminum alloy plates with the same set of method parameters:

- Welding Speed: 24 mm/min
- Rotational Speed: 1525 rpm
- Material of tool: [cold work tool steel A681 (D2) ASTM]
- Shoulder diameter: [20 mm]

In order to improve mechanical qualities, the second set has nano-Y_2O_3 reinforcement in the weld zone, whereas the first set was welded without it.

2.3 Analysis of microstructure

Grain refinement, phase distribution, and flaws in heat-affected zone (HAZ), thermo-mechanically affected zone (TMAZ), and nugget zone (NZ) were studied using optical microscopy. To illustrate the effect of nanoparticles on the quality of weld and mechanical qualities, pictures were taken comparing the grain size and morphology of nano-Y_2O_3-reinforced welds with non-reinforced welds.

2.4 Microhardness testing

A Vickers hardness tester was used to assess microhardness at a dwell time of 15 seconds and a force of 1.96 N. For both nano-reinforced and non-reinforced joints, the hardness values were measured at various weld sites.

2.5 Loading estimation justification

The loading conditions applied in the simulation including lift force (45.9375 N), drag force (1.53125 N), cyclic bending moment (5 Nm), centrifugal force (0.695 N), and weight (0.682 N) were designed to reflect idealized cyclic loading scenarios that may be encountered by lightweight structural components in aerospace environments. These values were estimated using simplified assumptions based on component mass, cross-sectional area, basic aerodynamic principles, and vibration-induced forces typical for small-scale assemblies such as stringers, panel stiffeners, or wing substructures. Although not derived from a specific aircraft load specification, these loads serve as reasonable proxies for evaluating comparative fatigue behavior between the nano-reinforced and non-reinforced welds.

2.6 Geometry creation

The geometry of two plates of AA2024 with 100 mm length, 50 mm width and 5 mm thickness. Modeled as a small strip along the plate contact, the weld zone is critical to FSW process with width 22 mm represents the diameter of tool shoulder. When nano-reinforcement is used, nano-Y_2O_3 particles are added to the weld zone's material properties. After that, the geometry is finely mesh to precisely capture stress distributions, especially in welding zone as shown in Figure 1 [31, 32].

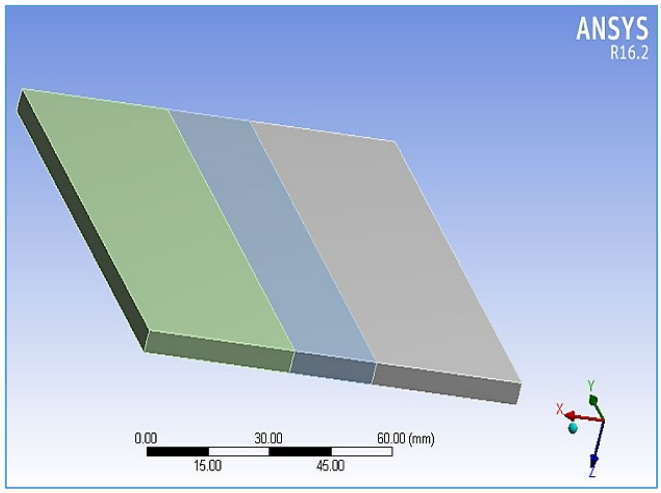

(a) Welding zone without mesh

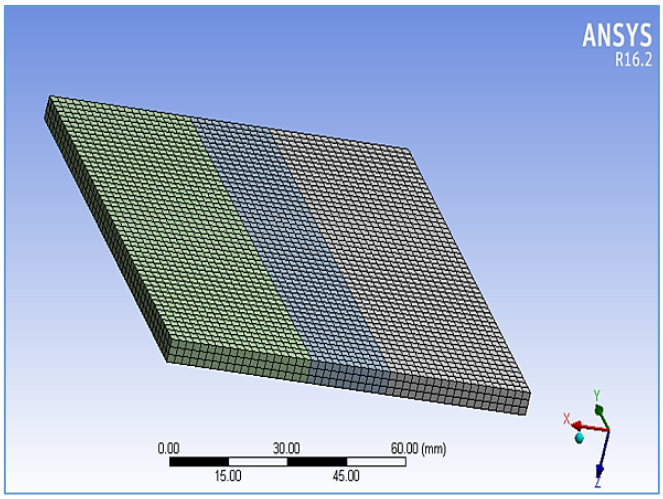

(b) Welding zone with mesh

Figure 1. Geometry creation

2.7 Finite element analysis setups

After the geometry was created and meshed, fatigue behavior of welded joints was simulated using finite element analysis (FEA) and ANSYS Workbench under the following loading conditions:

- Alternating Lift Force: 45.9375 N
- Alternating Drag Force: 1.53125 N
- Weight Force: 0.682 N
- Cyclic Bending Moment: 5 Nm
- Alternating Centrifugal Force: 0.695 N

The plates are subjected to applied loads at one end while being fastened at the other, to imitate attachment to a bigger structure. This configuration guarantees that the simulation accurately represents loading circumstances and offers a strong basis for further stress and analysis of fatigue life. For calculate the equivalent stresses and fatigue life for the nano-reinforced and non-reinforced welds, these forces were applied to the welded plates [33].

3. RESULTS AND DISCUSSION

3.1 Equivalent stress and fatigue life

FEA results show that welds without reinforcement had much higher stress concentrations than welds reinforced with nano-Y_2O_3. The SN curve study makes it clear that the reinforced joints' increased fatigue life was influenced by their enhanced capacity to support loads. The use of Y_2O_3 nanoparticles improved the grain structure, distributing stress more evenly and delaying the onset of cracks.

3.2 Observations on microstructure

Y_2O_3 has a beneficial effect on the microstructure, as seen by the visible grain refinement in the optical microscopy images of the weld nugget with nano-reinforcement as shown in Figure 2. The nano-reinforced welds showed the following characteristics in contrast to the unreinforced welds.

- Higher hardness is a result of finer grain structures in the stir zone.
- Reduced concentrations of localized stress due to a more consistent phase distribution.
- Reduced microstructural flaws, such voids and porosity, and improve resistance of fatigue.

The observed rise in the fatigue life and hardness values was directly correlated with these microstructural changes.

The enhanced fatigue life observed in nano-Y_2O_3-reinforced welds can be attributed to several interrelated microstructural mechanisms. The addition of Y_2O_3 nanoparticles promotes dynamic recrystallization during FSW, resulting in a finer, more homogeneous grain structure in the weld zone. Grain refinement reduces the effective slip length for dislocations and increases the number of grain boundaries, which influence as obstacles to propagation and beginning of the crack. Furthermore, the uniform dispersion of nanoparticles contributes to dislocation pinning, delaying the onset of fatigue damage. These mechanisms collectively suppress early-stage microcrack formation and contribute to the extended fatigue life observed in the numerical analysis. This relationship is supported by the optical microscopy results (Figure 2), which reveal a denser, more uniform microstructure in the reinforced weld.

(a) BM

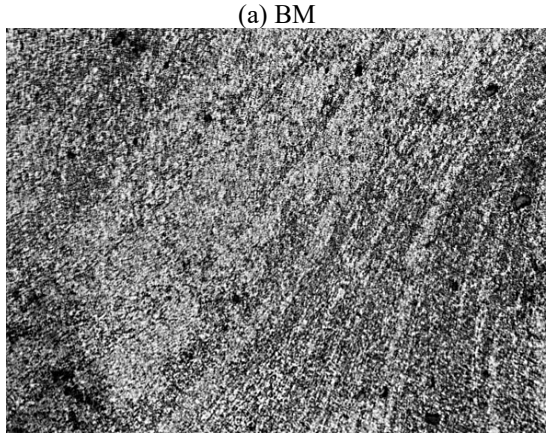

(b) Welding zones

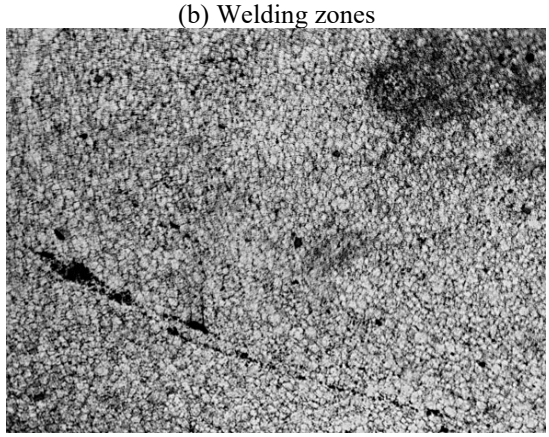

(c) NZ without nano-reinforced

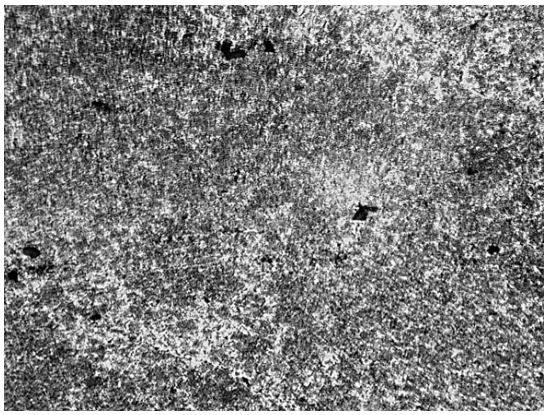

(d) NZ with nano-reinforced

Figure 2. Microstructure of AA2024/AA2024 weldments

3.3 Microhardness distribution analysis

The microhardness results show a significant variation in hardness in different weld areas as illustrated in Figure 3. Key points include:

- The strengthening effect of Y_2O_3 was confirmed by the up to 24% improvement in hardness in the NZ that nano-reinforced welds showed when compared to non-reinforced welds.
- The weld nugget, where nano-reinforcement had the biggest effect, had the highest hardness values.
- The nano-reinforced weld's HAZ and TMAZ areas showed a more progressive hardness change, which enhanced fatigue resistance.

The connection between microhardness and fatigue life suggests that higher hardness in a weld nugget helps to increase fatigue resistance by slowing down crack growth.

3.4 Equivalent stress analysis

Figure 4 illustrates the distribution of comparable stress for the FSW joint in absence of nano-Y_2O_3. According to the analysis, minimum stress is 0.016894 MPa, and maximum stress is 44.619 MPa. This stress distribution demonstrates, there are notable stress concentrations in the weld zone region of non-reinforced weld, which may cause an early failure under cyclic loading circumstances.

On the other hand, as illustrated in Figure 5, the corresponding stress distribution for FSW joint reinforced with nano-Y_2O_3 reveals a minimum stress of 0.0058662 MPa and a maximum stress of 44.638 MPa. Due to the improved microstructural qualities that the nano-Y_2O_3 particles give, the greater maximum stress indicates that the Nano-reinforced weld has a higher load-bearing capacity. Additionally, this distribution exhibits a more uniform stress gradient, which could be a factor in the better fatigue life seen in the analysis that follows.

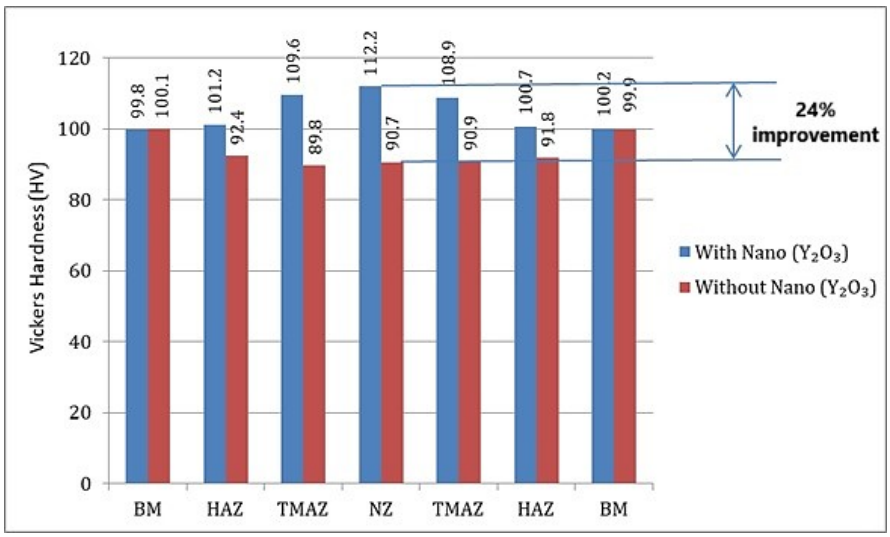

Figure 3. Hardness across BM, HAZ, TMAZ and NZ of AA2024/AA2024 weldments with and without nano particles

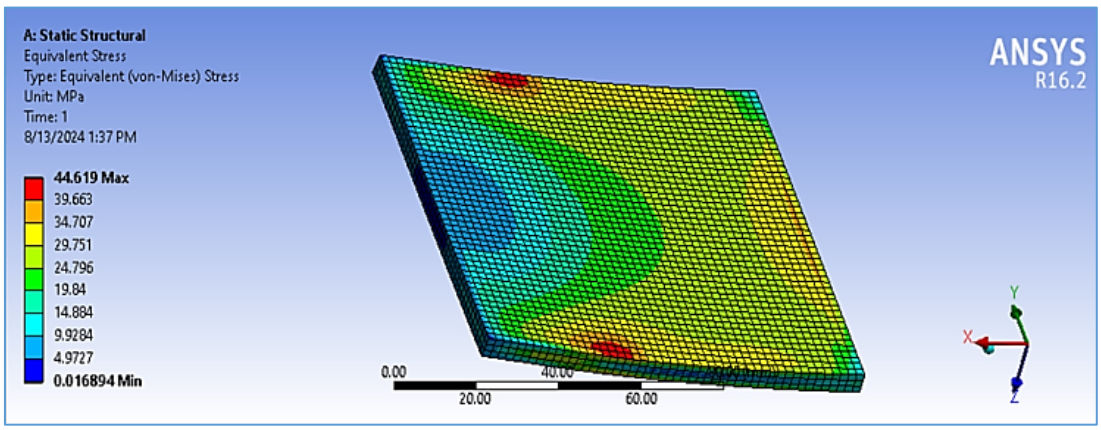

Figure 4. Equivalent stress distribution for FSW joint without nano

Although the maximum equivalent stress values for both the non-reinforced (44.619 MPa) and nano-reinforced (44.638 MPa) joints are numerically comparable, the main difference resides in the distribution of stress throughout the weld zone. In the reinforced joint, the high-stress area is more uniformly dispersed and less sharply focused, resulting in a smoother stress gradient. This redistribution of stress rather than a decrease in peak value suggests better mechanical performance by lessening local stress concentrations, which are usually the starting points for fatigue cracks. This observation aligns with the improved microstructure and microhardness measurements, backing the assertion of better fatigue life.

Figure 6 illustrated S-N curves produced for the non-reinforced and nano-reinforced welds. The fatigue life of the non-reinforced weld exhibits a sharp reduction with increasing stress amplitude, indicating the weld's susceptibility to fatigue failure [34, 35].

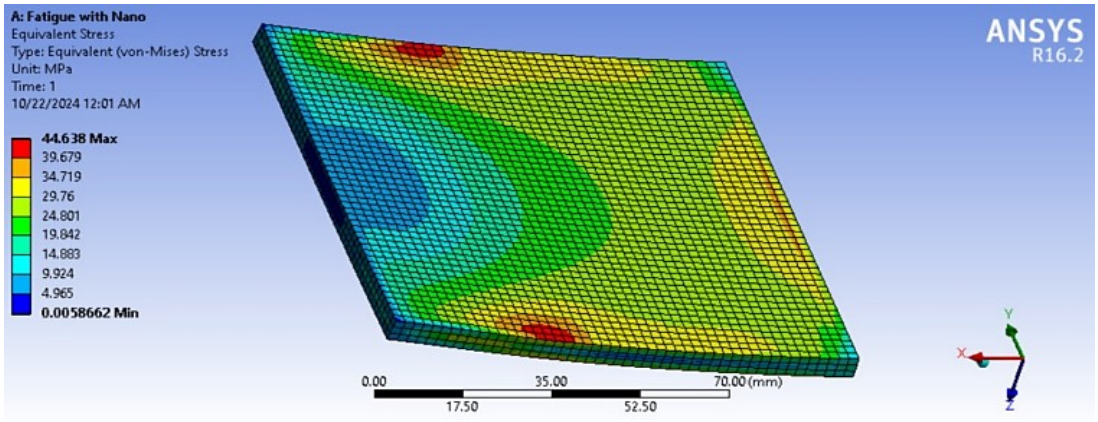

Figure 5. Equivalent stress distribution for the nano-Y_2O_3 reinforced FSW joint

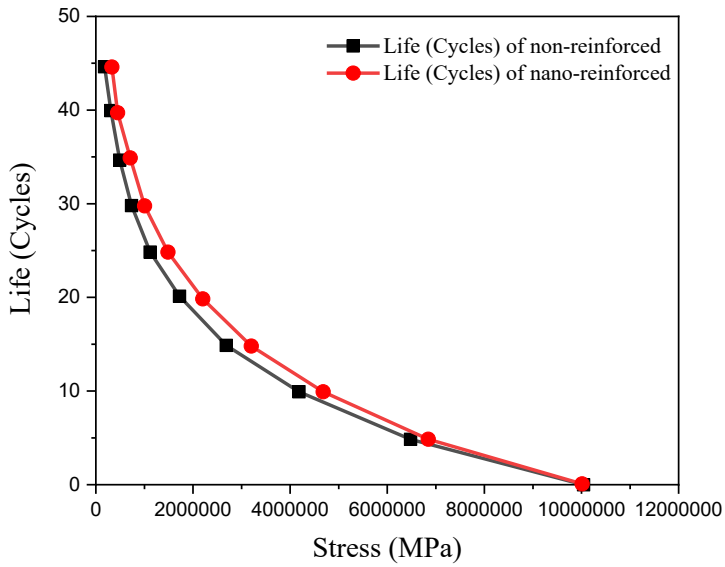

Figure 6. S-N curves comparing fatigue life of non-reinforced and nano-reinforced welds

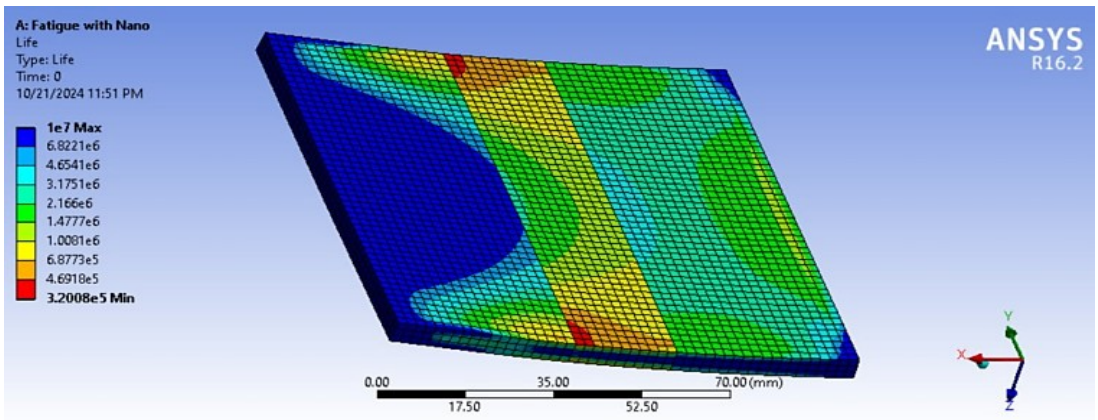

(a) Welds without nano

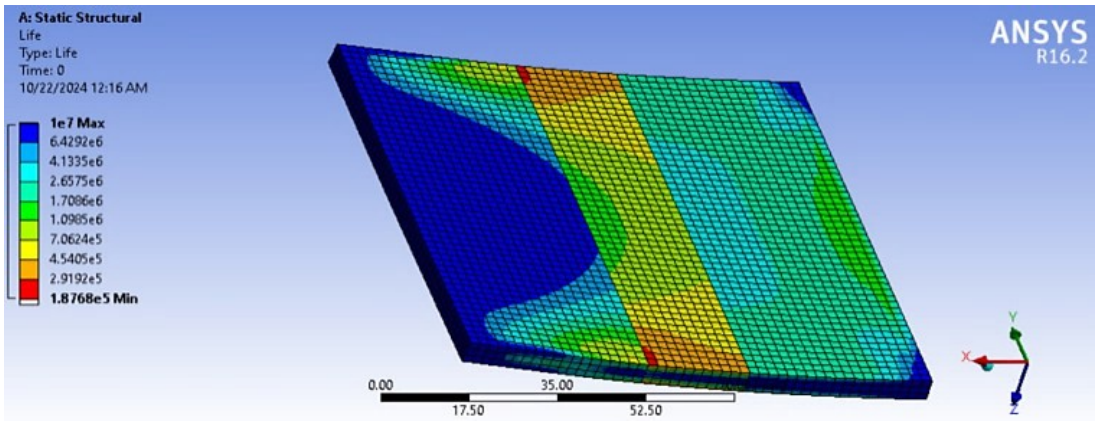

(b) Welds with nano

Figure 7. Fatigue life distribution showing maximum and minimum cycles

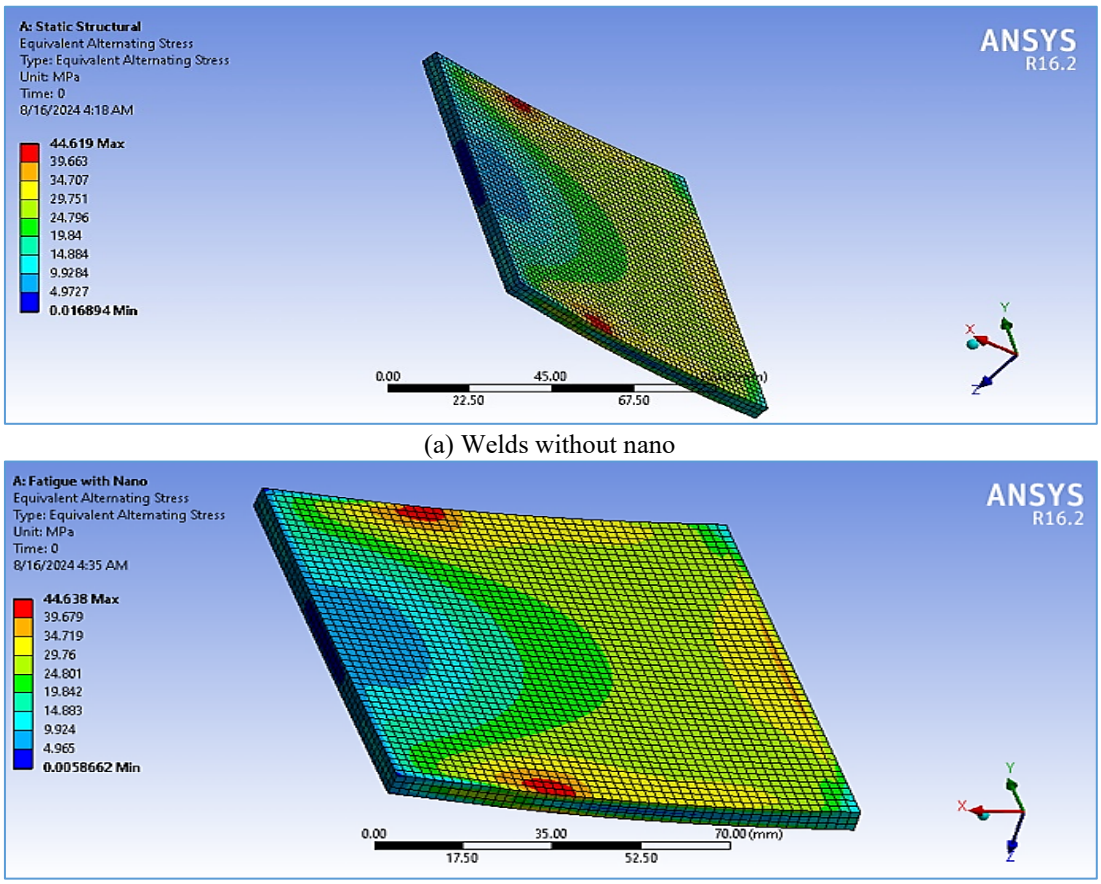

(a) Welds without nano

(b) Welds with nano

Figure 8. Representation of the applied cyclic bending moment and alternating forces, along with the resulting fatigue life distribution

3.5 Fatigue life analysis

Fatigue life data, as shown in Figure 7, show that the nano-reinforced and non-reinforced welds have a maximum life of 10,000,000 cycles. The minimum life of the nano-reinforced weld is 320,080 cycles, while the non-reinforced weld has a substantially minimum life of 187,680 cycles.

Based on the more favorable S-N curve features, addition of nano-Y_2O_3 particularly increases fatigue life of FSW joint by delaying beginning of cracks.

Figure 8 displays the fatigue life distribution that results from applying alternating stresses and cyclic bending moment to the welded plates.

The equivalent stress distribution over the welds shows notable stress concentrations at specific locations, as shown in Figures 4 and 5. The regions of decreased fatigue life in Figure 8. a show that these high-stress zones closely correlate to those where the application of cyclic bending moments and alternating loads exacerbates possible failure spots.

3.6 Correlation between equivalent stress and fatigue life

The analysis of the equivalent stress distributions, as shown in Figures 4 and 5, provides critical insight into the regions of the welded joints that are most susceptible to fatigue failure. These figures illustrate the stress concentration areas within

both the non-reinforced and nano-reinforced welded joints, with stress values significantly influencing the fatigue performance of the material.

The equivalent stress distributions directly correlate with the fatigue life results, as depicted in Figure 7. The regions identified with higher equivalent stress in Figures 4 and 5 correspond to the areas where the fatigue life is shortest, as presented in Figures 7 and 8. This direct relationship highlights that areas subjected to greater stress concentrations are more prone to early failure under cyclic loading conditions.

This correlation is critical for validating the simulation's accuracy. The fact that fatigue life distribution in Figure 8 mirrors the equivalent stress patterns in Figures 5 and 6, which supports the reliability of the equivalent stress as a predictor of fatigue life. The more uniform fatigue life distribution in the nano-reinforced weld suggests that the addition of nano-Y_2O_3 particles effectively mitigates stress concentrations, leading to improved fatigue resistance.

4. CONCLUSION

The integration of nano-Y_2O_3 particles into FSW processes has been shown to significantly enhance mechanical properties and the fatigue life of aluminum alloy 2024 welds. Microstructural analysis confirmed that Y_2O_3 nanoparticles refine grain structure, reduce micro-defects, and improve overall weld quality. These changes contributed to measurable increases in microhardness up to 25% and strengthened mechanical response under simulated cyclic loads.

FEA results demonstrated that fatigue life increased from 187,680 to 320,080 cycles (approximately 71%) in nano-reinforced welds. Although this improvement is substantial, it is important to clarify that fatigue predictions were based solely on numerical simulations. No experimental cyclic loading was performed in this study. However, the predicted trends are qualitatively supported by experimental findings, such as improved hardness and more homogeneous microstructure in the weld zone.

While increased hardness in the nano-reinforced welds provides a general indication of improved mechanical strength, fatigue resistance is more directly influenced by microstructural mechanisms. The refinement of grain size increases the number of grain boundaries, which influence as walls to dislocation motion and crack propagation. Moreover, the uniform dispersion of Y_2O_3 nanoparticles impedes crack growth by interrupting crack paths and redistributing localized stress. These microstructural features collectively suppress the initiation and progression of fatigue cracks, contributing to the enhanced performance predicted by the FEA.

Therefore, while the simulation suggests a strong potential benefit, further validation through experimental fatigue testing is essential and planned in future work. These findings highlight the potential of nano-Y_2O_3 as an effective reinforcement material in high-stress structural applications, particularly in aerospace environments where fatigue performance is critical. The study offers valuable insight into optimizing weld quality through nanotechnology, contributing to the advancement of lightweight and durable engineering components.

ACKNOWLEDGMENT

The authors would like to explain their sincere thankfulness to the laboratory staff and technical support team at Kut Technical Institution and University of Technology for their assistance in conducting the microhardness and microstructural tests.

REFERENCES

[1] Zhu, H., Li, J. (2024). Advancements in corrosion protection for aerospace aluminum alloys through surface treatment. International Journal of Electrochemical Science, 19(2): 100487. https://doi.org/10.1016/j.ijoes.2024.100487

[2] Ferreira, C.M., Reis, L., Carmezim, M.J., Cláudio, R. (2024). Additive manufacturing of aluminium alloys in the aeronautical sector–A bibliometric analysis. Procedia Structural Integrity, 53: 254-263. https://doi.org/10.1016/j.prostr.2024.01.031

[3] Polayya, C., Rao, C.S.P., Kumar, G.V. (2024). Improving the properties of aluminum-lithium composites in aerospace applications. Engineering Research Express, 6(2): 022501. https://doi.org/10.1088/2631-8695/ad3a37

[4] Razzaq, M.K.A., Abood, A.N. (2021). Effect of arc stud welding parameters on the microstructure and mechanical properties of AA6061 and AA5086 aluminium alloys. Journal of Achievements in Materials and Manufacturing Engineering, 108(1): 24-34. https://doi.org/10.5604/01.3001.0015.4796

[5] Ericsson, M., Sandström, R. (2003). Influence of welding speed on the fatigue of friction stir welds, and comparison with MIG and TIG. International Journal of Fatigue, 25(12): 1379-1387. https://doi.org/10.1016/S0142-1123(03)00059-8

[6] Bhudolia, S.K., Gohel, G., Leong, K.F., Islam, A. (2020). Advances in ultrasonic welding of thermoplastic composites: A review. Materials, 13(6): 1284. https://doi.org/10.3390/ma13061284

[7] Lionetto, F., Balle, F., Maffezzoli, A. (2017). Hybrid ultrasonic spot welding of aluminum to carbon fiber reinforced epoxy composites. Journal of Materials Processing Technology, 247: 289-295. https://doi.org/10.1016/j.jmatprotec.2017.05.002

[8] Cheng, X., Wang, S., Zhang, J., Huang, W., Cheng, Y., Zhang, J. (2017). Effect of damage on failure mode of multi-bolt composite joints using failure envelope method. Composite Structures, 160: 8-15. https://doi.org/10.1016/j.compstruct.2016.10.042

[9] Choi, J., Hasheminia, S.M., Chun, H.J., Park, J.C., Chang, H.S. (2018). Failure load prediction of composite bolted joint with clamping force. Composite Structures, 189: 247-255. https://doi.org/10.1016/j.compstruct.2018.01.037

[10] Huang, Y., Meng, X., Xie, Y., Wan, L., Lv, Z., Cao, J., Feng, J. (2018). Friction stir welding/processing of polymers and polymer matrix composites. Composites Part A: Applied Science and Manufacturing, 105: 235-257. https://doi.org/10.1016/j.compositesa.2017.12.005

[11] Zhou, C., Yang, X., Luan, G. (2006). Effect of root flaws on the fatigue property of friction stir welds in 2024-T3 aluminum alloys. Materials Science and Engineering: A, 418(1-2): 155-160. https://doi.org/10.1016/j.msea.2005.11.042

[12] Ahmed, M.M.Z., El-Sayed Seleman, M.M., Fydrych, D.,

Çam, G. (2023). Friction stir welding of aluminum in the aerospace industry: The current progress and state-of-the-art review. Materials, 16(8): 2971. https://doi.org/10.3390/ma16082971

[13] Kallee, S.W. (2001). Industrialisation of friction stir welding for aerospace structures. In Structures and Technologies-Challenges for Future Launchers, Third European Conference, Strasbourg, France, pp. 11-14.

[14] Wang, Q.Y., Lib, T., Zenga, X.G. (2010). Gigacycle fatigue behavior of high strength aluminum alloys. Procedia Engineering, 2(1): 65-70. https://doi.org/10.1016/j.proeng.2010.03.007

[15] Lemmen, H.J.K., Alderliesten, R.C., Benedictus, R. (2010). Fatigue initiation behaviour throughout friction stir welded joints in AA2024-T3. International Journal of Fatigue, 32(12): 1928-1936. https://doi.org/10.1016/j.ijfatigue.2010.06.001

[16] Mayer, H., Schuller, R., Fitzka, M. (2013). Fatigue of 2024-T351 aluminium alloy at different load ratios up to 10^{10} cycles. International Journal of Fatigue, 57: 113-119. https://doi.org/10.1016/j.ijfatigue.2012.07.013

[17] Yang, C., Wang, B.B., Yu, B.H., Wu, L.H., Xue, P., Zhang, X.M., He, G.Z., Ni, D.R., Xiao, B.L., Wang, K.S., Ma, Z.Y. (2020). High-cycle fatigue and fracture behavior of double-side friction stir welded 6082Al ultra-thick plates. Engineering Fracture Mechanics, 226: 106887. https://doi.org/10.1016/j.engfracmech.2020.106887

[18] Gaur, V., Enoki, M., Okada, T., Yomogida, S. (2018). A study on fatigue behavior of MIG-welded Al-Mg alloy with different filler-wire materials under mean stress. International Journal of Fatigue, 107: 119-129. https://doi.org/10.1016/j.ijfatigue.2017.11.001

[19] Leitner, M., Stoschka, M. (2020). Effect of load stress ratio on nominal and effective notch fatigue strength assessment of HFMI-treated high-strength steel cover plates. International Journal of Fatigue, 139: 105784. https://doi.org/10.1016/j.ijfatigue.2020.105784

[20] Pouget, G., Reynolds, A.P. (2008). Residual stress and microstructure effects on fatigue crack growth in AA2050 friction stir welds. International Journal of Fatigue, 30(3): 463-472. https://doi.org/10.1016/j.ijfatigue.2007.04.016

[21] Kim, S., Lee, C.G., Kim, S.J. (2008). Fatigue crack propagation behavior of friction stir welded 5083-H32 and 6061-T651 aluminum alloys. Materials Science and Engineering: A, 478(1-2): 56-64. https://doi.org/10.1016/j.msea.2007.06.008

[22] Singh, T. (2024). Effect of nanoparticles addition during friction stir welding of Al-FSW welds. Medicon Engineering Themes, 6(3): 1-3.

[23] Aldriasawi, S.K., Hasein, A.N., Anead, A.M., Mohamad, B. (2024). Investigation the effect of surface treatment on the mechanical properties of coating. Pollack Periodica, 19(2): 138-145. https://doi.org/10.1556/606.2024.00955

[24] Kumar, J.R., Jayaraman, M., Kumar, T.S., Priyadharshini, G.S., Kumar, J.S. (2019). Characterization of Y_2O_3 particles reinforced AA6082 aluminum matrix composites produced using friction stir processing, Materials Research Express, 6(8): 086509. https://doi.org/10.1088/2053-1591/ab19df

[25] Chen, J., Wen, F., Liu, C., Li, W., Zhou, Q., Zhu, W., Zhang, Y., Guan, R. (2021). The microstructure and property of Al–Si alloy improved by the Sc-microalloying and Y_2O_3 nano-particles. Science and Technology of Advanced Materials, 22(1): 205-217. https://doi.org/10.1080/14686996.2021.1891841

[26] Asl, N.S., Mirsalehi, S.E., Dehghani, K. (2019). Effect of TiO_2 nanoparticles addition on microstructure and mechanical properties of dissimilar friction stir welded AA6063-T4 aluminum alloy and AZ31B-O magnesium alloy. Journal of Manufacturing Processes, 38: 338-354. https://doi.org/10.1016/j.jmapro.2019.01.023

[27] Shehabeldeen, T.A., El-Shafai, N.M., El-Mehasseb, I.M., Yin, Y., Ji, X., Shen, X., Zhou, J. (2021). Improvement of microstructure and mechanical properties of dissimilar friction stir welded aluminum/titanium joints via aluminum oxide nanopowder. Vacuum, 188: 110216. https://doi.org/10.1016/j.vacuum.2021.110216

[28] Kamaleshwar, S., Jagadeesh Kumar, S., Naveen Kumar, K., Keerthana, S., Vaira Vignesh, R., Padmanaban, R. (2023). Investigations on the texture, formability, and corrosion characteristics of AA3003-Y_2O_3 surface composite fabricated by friction stir processing. In Advances in Processing of Lightweight Metal Alloys and Composites. Materials Horizons: From Nature to Nanomaterials. Springer, Singapore. https://doi.org/10.1007/978-981-19-7146-4_18

[29] Zhu, X.W., Deng, Y., Lai, Y., Guo, Y.F., Yang, Z.A., Fu, L., Xu, G.F., Huang, J.W. (2023). Effects of $Al_3(Sc_{1-x}Zr_x)$ nano-particles on microstructure and mechanical properties of friction-stir-welded Al-Mg-Mn alloys. Transactions of Nonferrous Metals Society of China, 33(1): 25-35. https://doi.org/10.1016/S1003-6326(22)66087-4

[30] Yaghoubi, M.A., Anjabin, N., Kim, H.S. (2023). Effect of Y_2O_3 nanoparticles on the evolution of the microstructure and mechanical properties of severely plastic deformed cu sheets during friction stir processing. Metals and Materials International, 29: 2710-2725. https://doi.org/10.1007/s12540-023-01398-7

[31] Akber, A.A., Khleif, A.A., Hasein, A.N. (2013). Friction stir welding of aluminum alloy 6063 pipe with aluminum alloy 7022 pipe. AIP Conference Proceedings, 2213: 020160. https://doi.org/10.1063/5.0000096

[32] Hasein, A.N. (2024). NDT for detecting imperfections of friction stir welding in two dissimilar aluminum alloys pipes (AA6082 and AA7022). AIP Conference Proceedings, 3105: 020019. https://doi.org/10.1063/5.0212239

[33] Hasein, A.N., Aned, A.M., Razzaq, M.K.A. (2023). Identifying some regularities of the heat transfer in the welded joint of sus304 pipe using a numerical approach. Eastern-European Journal of Enterprise Technologies, 5(1(125): 104-113. https://doi.org/10.15587/1729-4061.2023.290124

[34] Long, L., Zhang, X., Gu, S., Li, X., Cheng, X., Chen, G. (2024). Experimental and simulation investigation on fatigue performance of H13 steel tools in friction stir welding of aluminum alloys. Materials, 17(7): 1535. https://doi.org/10.3390/ma17071535

[35] Wang, X., Guo, X., Li, X., Ge, D. (2014). Improvement on the fatigue performance of 2024-T4 alloy by synergistic coating technology. Materials, 7(5): 3533-3546. https://doi.org/10.3390/ma7053533

NOMENCLATURE

AA2024	Aluminum Alloy 2024
FSW	Friction Stir Welding
Y_2O_3	Yttrium Oxide
FEA	Finite Element Analysis
S-N Curve	Stress-Number of Cycles Curve
MPa	Megapascal (Unit of Stress)
N	Newton (Unit of Force)
Nm	Newton-Meter (Unit of Torque or Moment)
IACS	International Annealed Copper Standard
N_f	Fatigue Life, Cycles
F_lift	Alternating Lift Force, N
F_drag	Alternating Drag Force, N
F_weight	Weight Force, N
M_bending	Cyclic Bending Moment, Nm
F_centrifugal	Alternating Centrifugal Force, N
BM	Base Metal
HAZ	Heat Affected Zone
TMAZ	Thermo-Mechanically Affected Zone
NZ	Nugget Zone

Greek symbols

E	Young's Modulus (Elastic Modulus), GPa
ρ	Density, g/cm³
σ_eq	Equivalent Stress, MPa
σ_max	Maximum Stress, MPa
σ_min	Minimum Stress, MPa